Journal of the Mechanical Behavior of Biomedical Materials 175 (2026) 107318

Contents lists available at ScienceDirect

Journal of the Mechanical Behavior of Biomedical Materials

journal homepage: www.elsevier.com/locate/jmbbm

Evaluation of a novel 4-day decellularisation protocol for porcine flexor tendons: A comparative study with a 26-day process

Victoria Haines [a,b,*], Jennifer Helen Edwards [b], Anthony Herbert [a]

[a] Institute of Medical and Biological Engineering, School of Mechanical Engineering, Faculty of Engineering and Physical Sciences, University of Leeds, Leeds, United Kingdom

[b] Institute of Medical and Biological Engineering, School of Biomedical Sciences, Faculty of Biological Sciences, University of Leeds, Leeds, United Kingdom

ARTICLE INFO

Keywords:
Decellularisation
Tendon
Anterior cruciate ligament
Biomechanics
Tissue engineering

ABSTRACT

Rupture of the anterior cruciate ligament is a common sports-related injury that lacks intrinsic healing capacity, often necessitating surgical intervention. Our group has developed a new graft biomaterial, the decellularised porcine super flexor tendon (pSFT), designed to mitigate immune rejection post-implantation by removing cellular components. The current 26-day decellularisation process attenuates the mechanical properties of the graft, potentially disrupting the structural micro-cues that influence cell repopulation and integration. This study investigates a shortened 4-day protocol to determine whether mechanical properties are preserved more closely to native, unprocessed tissue.

Histological analysis and DNA quantification confirmed effective cell removal for both the 26-day and 4-day protocols. Native, 26-day processed, and 4-day processed grafts were mechanically evaluated through stress relaxation and failure testing. Following stress relaxation testing, several Maxwell-Weichert viscoelastic parameters were found to significantly differ between 26-day and native groups (E_0, E_1, E_2 & τ_2), whereas between 4-day and native groups fewer significant differences were found (E_1 & E_2). Following failure testing, again several parameters were found to significantly differ between 26-day and native groups (P_{FAIL}, UTS, E_{linear} and ε_T), whereas between 4-day and native groups only one parameter was significantly different (E_{linear}).

These findings indicate that the 4-day decellularisation process better preserves the native tissue mechanical properties, potentially reducing structural alterations and improving suitability for anterior cruciate ligament replacement.

1. Introduction

Rupture of the anterior cruciate ligament (ACL) has an annual incidence of approximately 0.08 % in the general population (Solis-Cordova et al., 2023; Zbrojkiewicz et al., 2018; Maniar et al., 2022; Nordenvall et al., 2012) and can be as high as 4 % in those undertaking professional sport (Saueressig et al., 2022). Natural healing can be difficult to achieve and surgery is usually required using a replacement graft material (Solis-Cordova et al., 2023; Edwards et al., 2021). According to a 2022 report by the UK National Ligament Registry, the most popular graft choice in the UK is hamstring tendon autograft (The_National_Ligament_Registry and The Seventh Annual Report, 2022), with positive results in restoring return to daily activities and sport. There are however disadvantages, including the need for two surgical sites and some patients reporting donor site morbidity (Solis-Cordova et al., 2023; Herbert et al., 2015; Legnani and Ventura, 2023). Allografts are also used, however these are likely to be taken from older donors, have reduced mechanical properties and present the risk of disease transmission (Noyes and Grood, 1976; Woo et al., 1991; Nordin and Frankel, 2022). Synthetic grafts are not commonly used, with several products being withdrawn from the market due to side effects including high failure rate, inflammatory response in surrounding tissues, osteoarthritis and wear debris found in other areas of the body (Legnani and Ventura, 2023; Marieswaran et al., 2018).

There is a need for a new off-the-shelf graft that can restore joint function and biologically integrate with the host without the limitations of current graft options. Our group has developed a decellularised tendon graft, utilising the porcine super flexor tendon (pSFT) of the pig

* Corresponding author. Institute of Medical and Biological Engineering, School of Mechanical Engineering, Faculty of Engineering and Physical Sciences, University of Leeds, Leeds, LS2 9JT, United Kingdom.

E-mail addresses: mn22vkhw@leeds.ac.uk (V. Haines), J.H.Edwards@leeds.ac.uk (J.H. Edwards), a.herbert@leeds.ac.uk (A. Herbert).

https://doi.org/10.1016/j.jmbbm.2025.107318
Received 10 July 2025; Received in revised form 1 December 2025; Accepted 18 December 2025
Available online 19 December 2025

foot (Herbert et al., 2015). The decellularisation process removes the native cells and genetic material that would otherwise cause a negative immune response and facilitates the population of the remaining scaffold with host cells. Studies by our group of decellularised pSFT to date have investigated the introduction of fat and bioburden reduction process steps (Herbert et al., 2015), the static and dynamic material properties (Edwards et al., 2019), glycosaminoglycan content and bi-phasic compressive properties (Solis-Cordova et al., 2023), functional stratification (Whitaker et al., 2019), sterilisation approaches (Edwards et al., 2017; Herbert et al., 2017) and in-vivo implantation in mice (Jones et al., 2017) and sheep (Edwards et al., 2021), with the length of the decellularisation process ranging between 24 and 30 days long. These studies used similar process steps including the use of acetone, hypotonic buffer with low concentration sodium dodecyl sulfate (0.1 % w/v SDS), nuclease washes, and various sterilisation techniques including antibiotics, peracetic acid and irradiation. In one study, chloroform-methanol was explored as an alternative fat reducing agent to acetone (Herbert et al., 2015). Uniquely, our group utilises low concentration SDS to minimise microstructural damage to tissues (Moffat et al., 2022) whilst sufficiently removing nuclear material, resulting in a gentle and long process.

Other groups have decellularised rabbit semitendinosus (Dong et al., 2015), equine flexor (Aeberhard et al., 2020), and porcine achilles (Dede Eren et al., 2020) tendon tissue, with the decellularisation process length ranging from 2 days for tendon slices (Aeberhard et al., 2020) and 19 days for achilles tendon (Dede Eren et al., 2020). Therefore, the average process length is difficult to determine due to the difference in the size of tissue. Process steps also varied, including the use of SDS 1 %, trypsin, Triton X-100, sodium hydrogen carbonate, tributyl phosphate 1 % and polysorbate 20 1 % (Dong et al., 2015; Aeberhard et al., 2020; Dede Eren et al., 2020).

Previous research by the group have found changes to pSFT mechanical properties following decellularisation, with the viscoelastic properties being particularly affected (Solis-Cordova et al., 2023; Herbert et al., 2015; Edwards et al., 2019). Structural alterations of the extracellular matrix are likely to alter the micro physical and chemical cues of the tissue which have been shown to encourage cell migration and proliferation (Moffat et al., 2022).

It is hypothesised that a new shorter decellularisation process will better preserve the mechanical properties of the native source tissue. A shorter process may also be more cost effective and provide opportunities for large-scale automated manufacture.

A proposed new 4-day process will continue to use a low concentration SDS solution whilst addressing the use of harsher chemicals and reducing the length of steps where possible. The existing 26-day process uses acetone, which has been shown to be disruptive to the source tissue, causing dehydration and altering stiffness (Moffat et al., 2022). The 4-day process will remove acetone in addition to antibiotic and peracetic acid process steps, collectively replacing these with isopropanol. This study will examine the biomechanical effects of the 26- and 4-day decellularisation processes on pSFTs in comparison to native, unprocessed controls.

2. Materials and methods

2.1. Tissue sourcing and allocation

The hind legs of 3–6 month old, Large White pigs were obtained from an abbatoir (J. Pennys, Leeds), stored in chilled conditions within 3 days of sacrifice. pSFT's were removed from the posterior of the foot and ankle and stored on filter paper moistened with phosphate buffered saline (PBS) at −20 °C until the day of testing (up to 6 weeks). pSFT's harvested had a mean cross-sectional area of 42.3 mm^2 (range 38.1–47.5 mm^2) and an approximate length of 130 mm.

pSFT's were allocated to three groups (n = 6 in all cases):

- Native unprocessed
- 26-day decellularised
- 4-day decellularised

2.2. Decellularisation

2.2.1. 26-Day decellularisation process

pSFT's allocated to the 26-day decellularisation process were frozen overnight at −20 °C in falcon tubes in 50 ml hypotonic buffer including protease inhibitors (10 mM tris [Sigma-Aldrich], 2.7 mM EDTA [Fisher Scientific], 10 $KIU.mL^{-1}$ aprotinin [Nordic Pharma]). The tendons were thawed, hypotonic replaced and frozen at −20 °C over the weekend. All further washes were incubated at 42 °C with agitation at 220 rpm unless noted otherwise. Tendons were washed in 50 ml acetone [VWR International] for 3 × 1 h with 10 min sonication at the end of each wash. Tendons were then washed in 50 ml PBS with 10 $KIU.mL^{-1}$ aprotinin [Nordic Pharma] for 5 × 5 min. Tendons were transferred to 150 ml individual pots with 100 ml solution. Tendons were washed in an antibiotic wash solution (PBS containing 0.05 mg ml^{-1} vancomycin [Sigma], 0.5 mg ml^{-1} gentamicin [Merck] and 0.2 mg ml^{-1} Polymyxin B [Merck]) at 37 °C for 1 h, and then in hypotonic buffer with aprotinin overnight with sonication for the last 10 min. Subsequent washes were SDS hypotonic buffer with aprotinin (0.1 % w/v SDS [Fisher Scientific], 10 mM tris [Sigma-Aldrich], 2.7 mM EDTA [Fisher Scientific], 10 $KIU.mL^{-1}$ aprotinin [Nordic Pharma]) overnight, hypotonic buffer with aprotinin overnight and SDS hypotonic buffer with aprotinin overnight. Tendons were then washed in PBS containing aprotinin for 3 × 30 min, a wash over the weekend and then 1 × 30 min. Tendons were then incubated in 50 ml nuclease working solution (50 mM tris [Sigma-Aldrich], 1 mM $MgCl_2$ [Sigma-Aldrich], 10 $U.mL^{-1}$ Benzonase [Merck]) at 37 °C with agitation at 80 rpm for 3 × 2 h. Following washes included PBS for 3 × 30 min, hypertonic buffer (50 mM tris [Sigma-Aldrich], 1.5 M sodium chloride [Fisher Scientific]) overnight, PBS for 3 × 30 min and overnight. Tendons were then washed in peracetic acid treatment (0.1 % (v/v) solution of peracetic acid [Sigma-Aldrich] in PBS) at 27 °C for 3 h. Finally, the tendons were washed in PBS for 3 × 30 min, once for 48 h, over the weekend and for a week. On the last day the tendons were drained and frozen at −20 °C. The sequence of steps used in the 26-day decellularisation process are illustrated in Fig. 1a.

2.2.2. 4-Day decellularisation process

pSFT's allocated to the 4-day decellularisation process were initially thawed and then frozen at −20 °C in falcon tubes in 50 ml hypotonic buffer (10 mM tris [Sigma-Aldrich], 2.7 mM EDTA [Fisher Scientific]) for a minimum of 3 h. All further washes were incubated at 42 °C with agitation at 220 rpm unless noted otherwise. The tendons were thawed and subject to washes in 50 ml isopropanol [Fisher Scientific] for 2 × 1 h. Tendons were transferred to 150 ml individual pots with all further washes using 100 ml solution unless noted otherwise. Washes included hypotonic buffer for 1.5 h, hypotonic buffer with SDS (0.1 % w/v SDS [Fisher Scientific], 10 mM tris [Sigma-Aldrich], 2.7 mM EDTA [Fisher Scientific]) for 1 h, and hypotonic buffer with SDS overnight. Tendons were washed in PBS three times for 5–15 min and then incubated in 80 ml nuclease working solution (50 mM tris [Sigma-Aldrich], 1 mM $MgCl_2$ [Sigma-Aldrich], 10 $U.mL^{-1}$ Benzonase [Merck]) with agitation at 80 rpm for 2 × 2.5 h. Subsequently the tendons were washed in PBS three times for 5–15 min, and hypertonic buffer (50 mM tris [Sigma-Aldrich], 1.5 M sodium chloride [Fisher Scientific]) overnight. The next day washes included PBS for 1 h, hypertonic buffer for 1 h, PBS for 1 h, PBS for 2 x 5–15 min and then PBS overnight. On the last day the tendons were drained and frozen at −20 °C until the day of testing. The sequence of steps used in the 4-day decellularisation process are illustrated in Fig. 1b.

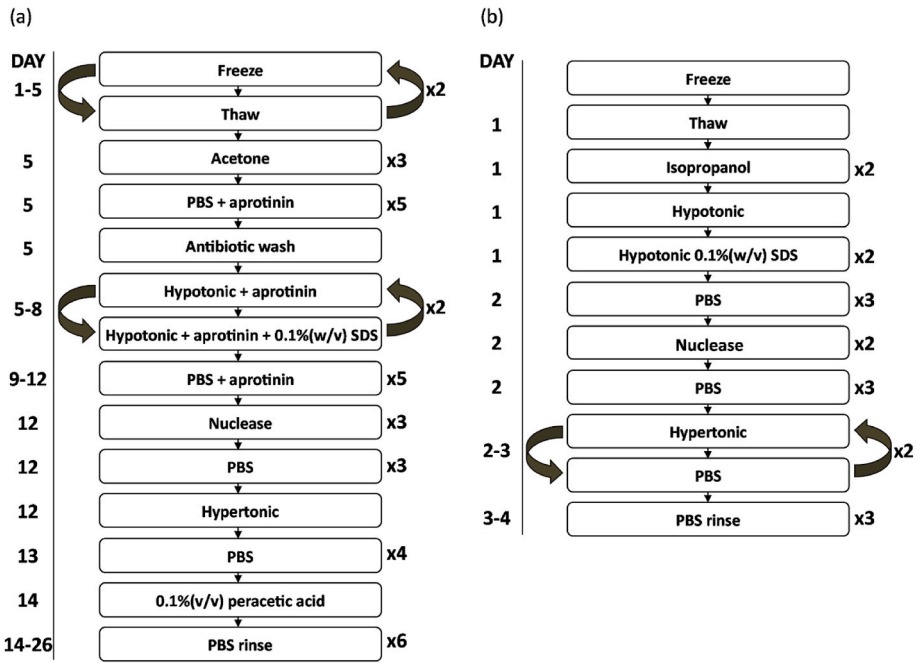

Fig. 1. The sequence of steps used in decellularising pSFTs (a) the 26-day decellularisation process and (b) the 4-day decellularisation process.

2.3. Histological evaluation

Transverse samples taken from all 18 tendons were fixed using a tissue processor (Leica), in 10 % (v/v) neutral buffered formalin (NBF) for 22 h. Samples were embedded in paraffin wax using standard techniques. 8 μm sections were taken from each specimen block and stained with hematoxylin [Atom Scientific] and eosin [VWR] (H & E), 4',6-diamidino-2-phenylindole [Merck] (DAPI) and Direct Red 80 [VWR] and picric acid [Sigma-Aldrich] (Picro-Sirius Red). An upright microscope Carl Zeiss Axio Imager M2 with Axio Cam MRc5 using Zen Pro 2012 software was used to view H & E, DAPI and Picro-Sirius Red slides. Bright-field illumination was used to image H & E, fluorescent illumination for DAPI, and polarised light for Picro-Sirius Red.

2.4. DNA quantification of native and decellularised pSFTs

The DNA content was measured using one sample taken from each tendon. Samples were extracted for native (n = 6), 26-day process group (n = 6) and 4-day process group (n = 6), minced and then weighed (20–30 mg native tissue and 200–250 mg decellularised tissue). Samples were freeze-dried until the weight stabilised and peqGOLD Blood & Tissue DNA Mini Kit [VWR] was used to extract DNA following the manufacturer's instructions. DNA concentrations were quantified by adding PicoGreen stock [from Quant-iT PicoGreen dsDNA Assay Kit] to standards and samples. Fluorescence was measured using a Hidex Chameleon Microplate Reader. DNA standards were plotted and the linear trendline gradient was used to convert reading of unknown samples to DNA concentrations.

2.5. Biomechanical testing

2.5.1. Specimen preparation

All tendons were thawed to room temperature and cut to 100 mm lengths. The tendons were snap frozen with dry ice and then processed with a scalpel to a dumbbell shape with gauge length of 30 mm and cross-sectional area of 3.5 mm by the natural specimen thickness (range 4.0–6.4 mm, mean 4.8 mm) (Herbert et al., 2015). The specimens were then stored on filter paper moistened with PBS at −20 °C until the day of testing.

Tendons were thawed at room temperature for 1 h. Immediately prior to mechanical testing, the specimen width and thickness were measured at three locations along the specimen gauge length using digital Vernier calipers. Average values of thickness and width were used to calculate the cross-sectional area of specimens.

2.5.2. Stress relaxation testing

A previous protocol for stress relaxation testing used by our group (Herbert et al., 2017) was employed for this study. Bespoke grips were used to mount the specimens on an Instron 3365 (Instron, Bucks, UK) materials testing machine equipped with a 500 N load cell. A tensile pre-load of 0.5 N was applied, followed by ten preconditioning cycles between 0 and 5 % strain at a rate of 15 mm/min. Tensile extension was then applied at a rate of 30 mm/min until a stress of 5 MPa was reached, at which point the tissue was then held at the corresponding extension for a period of 300 s allowing stress relaxation to occur. Previous studies have showed this stress value to be a physiological relevant tensile load in the ACL of the human knee (Hosseini et al., 2011; Shelburne et al., 2004). All data was recorded at a frequency of 50 Hz.

Engineering stress, σ, was calculated by dividing the force recorded by the load cell by the initial cross-sectional area of the specimen. Engineering strain, ε, was calculated by dividing the applied extension by the initial gauge length of the specimen (30 mm).

The relaxation modulus, $E(t)$, was calculated using the following relationship:

$$E(t) = \frac{\sigma(t)}{\varepsilon}$$

The data was then fitted to a modified Maxwell-Weichert viscoelastic model (Herbert et al., 2015; Jimenez Rios et al., 2007), with non-linear least squares method ($r^2 > 0.97$):

$$E(t) = E_0 + \frac{1}{t_0}\sum_{i=1}^{n} E_i \tau_i \exp^{-\frac{t}{\tau_i}}\left(\exp^{\frac{t_0}{\tau_i}} - 1\right)$$

The coefficients determined were a time-independent elastic modulus, E_0, time-dependent elastic moduli, (E_i) and relaxation times, (τ_i). The model chosen was single spring in parallel with 2 Mx elements (second order, i.e. n = 2).

2.5.3. Failure testing

Following stress relaxation testing the tendons were left to rest at room temperature wrapped in PBS soaked filter paper for a minimum of 2 h. Failure testing was performed using a previous protocol employed by our group (Herbert et al., 2015; Edwards et al., 2017; Jones et al., 2017). In this instance, the Instron 3365 was equipped with a 5 kN load cell and the bespoke grips were filled with dry ice using the principles of cyroclamps (Riemersa and Schamhardt, 1982) to accommodate the additional tensile loads specimens would experience. A 0.5 N pre-load was applied, followed by ten preconditioning cycles between 0 and 5 % strain at a rate of 15 mm/min. A tensile ramp was then applied at a rate of 30 mm/min until mid-substance failure occurred. Data was recorded at a frequency of 50 Hz.

The maximum force (P_{FAIL}) and extension at failure (δ_{FAIL}) were recorded to calculate the ultimate tensile strength (*UTS*) and strain at failure (ε_{FAIL}).

Engineering stress and strain were fitted to the following bi-linear model using a custom written Matlab R2020a programme (Herbert et al., 2016):

$$\sigma = E_{toe} \cdot \varepsilon \text{ for } \varepsilon \leq \varepsilon_T$$

$$\sigma = E_{linear} \cdot \varepsilon + c \text{ for } \varepsilon > \varepsilon_T$$

This model uses non-linear least squares regression to calculate the elastic modulus of the toe region, E_{toe}, and the linear region, E_{linear}. ε_T and σ_T represent the coordinates of the transition point between toe and linear regions, where ε_T is the transition strain, σ_T is the transition stress and c is a constant.

2.5.4. Statistical analysis

Minitab Statistical Software 21.4.1.0 was used to perform statistical analysis. Following a Ryan-Joiner test to demonstrate normality, a one-way analysis of variance (ANOVA) data analysis was performed to investigate for the presence of statistical variances between groups. The Tukey post-hoc method was employed to determine significant differences between group pairings. A p-value of <0.05 was considered significant.

3. Results

3.1. Histological analysis

Native tendon sections histologically stained with H & E and DAPI (Fig. 2 A, D) revealed the presence of cells and nuclei, with large clusters in the endotenon channels. H & E and DAPI staining of the 26-day group (Fig. 2 B, E) demonstrated no presence of cellular material. H & E staining of the 4-day group (Fig. 2. C) indicated no presence of cellular material. DAPI staining of the 4-day group (Fig. 2. F) indicated no cellular material in the majority of the tissue, however there was some evidence of residual material in the epitenon region (indicated with arrows), although no whole cell nuclei were visible.

Picro-Sirius Red staining was employed to visualise collagen fibres. Across all experimental groups, collagen exhibited both red and green birefringence; however, the native tissue showed a higher proportion of green colouration (Fig. 2. G). The 26-day and 4-day groups demonstrated a marked shift towards greater proportions of red colouration (Fig. 2 H, I).

3.2. DNA quantification

The native porcine super flexor tendon had a DNA quantity level of 419 ± 113 ng/mg per tissue dry weight (mean ± 95 % confidence

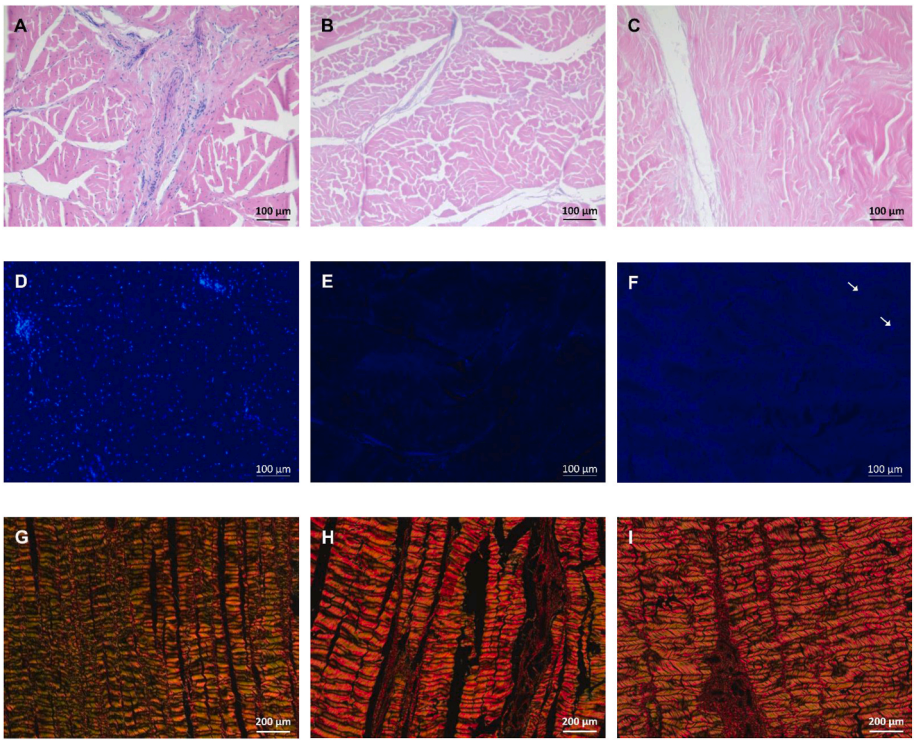

Fig. 2. Histological sections of porcine super flexor tendons: native (**A, D, G**), 26-day decellularisation group (**B, E, H**), and 4-day decellularisation group (**C, F, I**). Sections stained with hematoxylin and eosin (H & E) (**A–C**) show blue-stained nuclei present in the native tissue (**A**), but absent in both decellularised groups (**B, C**). Sections stained with 4′,6-diamidino-2-phenylindole (DAPI) (**D–F**) show bright white nuclear staining in native tissue (**D**), with no nuclei visible in decellularised samples (**E, F**). Minor residual cellular material was observed in the epitenon of the some 4-day decellularised samples (**F** – indicated with arrows). Sections stained with Picro-Sirius Red (**G–I**) show collagen with green and red colouration. H & E and DAPI images captured at 10x magnification (scale bar 100 µm). Picro-Sirius Red images captured at 5x magnification (scale bar 200 µm). (For interpretation of the references to colour in this figure legend, the reader is referred to the Web version of this article.)

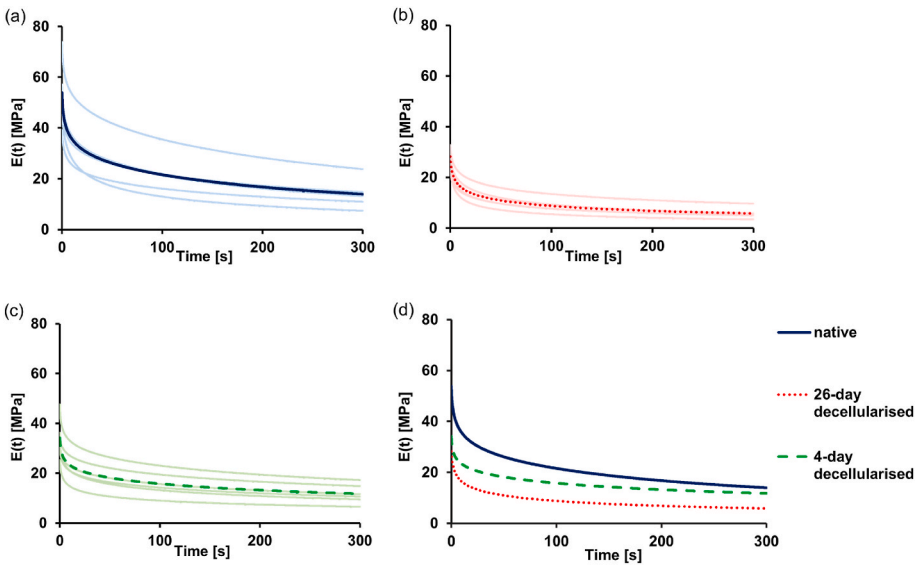

Fig. 3. Relaxation modulus profiles obtained during stress relaxation testing for **(a)** native, **(b)** 26-day decellularised and **(c)** 4-day decellularised pSFT groups (n = 6 in all cases). All specimen curves for each group are shown with the mean curve highlighted in bold. **(d)** The mean curves are reproduced in isolation to compare groups.

interval). Following decellularisation, the 4-day group had a mean of 48 ± 13 ng/mg and the 26-day group a mean of 45 ± 7 ng/mg per tissue dry weight.

3.3. Biomechanical testing

3.3.1. Stress relaxation testing

The mean relaxation modulus profiles for each of the three groups investigated are presented in Fig. 3. The 26-day group profile appears to be markedly different from the native profile, with the relaxation modulus remaining considerably lower at the end of the relaxation period. The 4-day group profile is more similar to the native profile, although differences are still apparent, particularly in the early stages of the relaxation period. The 4-day group relaxation modulus is similar to the native group at the end of the relaxation period.

The parameters determined from the modified Maxwell-Wiechert model are presented in Table 1.

3.3.2. Failure testing

The mean stress-strain profiles for each of the three groups investigated is presented in Fig. 4. The profiles of the 26-day and 4-day decellularised groups have more shallow gradients in their linear regions than the native group, and both have lower UTS values than the native group.

The parameters determined by fitting the bi-linear model to the stress-strain data are presented in Table 2.

4. Discussion

The findings of the study prove the hypothesis that a shorter decellularisation process of 4 days, with reduced wash times, using more gentle chemical agents, better preserves the mechanical properties of the native pSFT than the 26-day decellularisation process.

Histological assessment confirmed the absence of intact cell nuclei in the decellularised groups, although some residual material was observed in the epitenon region of the 4-day group. DNA quantification revealed that both the 26-day and 4-day decellularised groups contained double stranded DNA levels of less than 50 ng/mg, which falls within the recommended threshold for decellularised biological tissue (Crapo et al., 2011; Hussein et al., 2018). This indicates that the 4-day group is sufficiently decellularised; however, further investigation is required to determine whether the residual material affects cell migration and proliferation.

Histological analysis using Picro-Sirius Red staining was performed to visualise collagen fibres under polarised light. This technique enhances birefringence, producing colour variations that are considered indicative of differences in collagen type, fibre thickness, alignment, and packing density (Dayan et al., 1989; Junqueira et al., 1979; Liu et al., 2021). The staining revealed a reduction in green birefringence in both the 4-day and 26-day groups compared to native tissue. It is unclear whether this reduction reflects a decrease in type III collagen (Junqueira et al., 1979; Liu et al., 2021), an increase in fibre thickness (Dayan et al., 1989) associated with the decellularisation process, or alterations in fibre packing and alignment (Dayan et al., 1989). Additionally, Picro-Sirius Red staining provided insight into fibre crimp morphology. The native group exhibited a smooth and consistent crimp pattern, whereas the 26-day group appeared to have less consistency with some larger crimp periods. The crimp period in the 4-day group appears more comparable to that of the native group than to the 26-day group. Further high-resolution microscopic analysis is required to confirm these observations.

The non-linear time-dependent behaviour of the tendons due to their inherent viscoelastic nature (Woo et al., 1991), was measured through stress relaxation testing in tension. The tendon was held at a fixed displacement with the stress reduction over a fixed period observed, replicating flexion and positional hold of the knee. Following the stress relaxation testing it was found that both decellularisation processes affected the viscoelastic properties of the specimens. The mean relaxation modulus profiles for both decellularised groups were noticeably different to the native, however the 4-day group appeared less affected than the 26-day group (Fig. 3.). Following application of the Maxwell-Wiechert model, the 26-day group had four out of five viscoelastic parameters significantly different to the native, E_0, E_1, E_2 and τ_2 (Table 1), which is consistent with previous findings by the group (Herbert et al., 2015). The 4-day group had two out of five viscoelastic parameters significantly different to the native, the time-dependent moduli E_1 and E_2 (Table 1). Following decellularisation, tissues will likely become more porous and the viscosity associated with interstitial fluid flow will decrease. Therefore changes to the time-dependent moduli, E_1, E_2 are not surprising and the increased porosity could ultimately be beneficial in aiding population with endogenous cells. The time-independent elastic modulus, E_0 is thought to be representative of

Table 1
Stress relaxation parameters determined from the modified Maxwell-Wiechert model for native, 26-day and 4-day decellularised pSFT groups. All data is presented as mean ± 95 % confidence intervals (n = 6). Data was analysed using a one-way ANOVA with Tukey post-hoc test to determine significant differences ($p < 0.05$). Groups not sharing the same superscript letter within each column are significantly different. Values in round brackets indicate p-values when 26- and 4-day decellularised groups are compared to the native group. Values in square brackets indicate p-values when comparing 26- and 4-day decellularised groups.

Group	E_0 [MPa]	E_1 [MPa]	E_2 [MPa]	τ_1 [s]	τ_2 [s]
Native	12.30 ± 3.56[a]	10.05 ± 1.95[a]	20.35 ± 4.65[a]	7.45 ± 0.40[a]	124.54 ± 12.62[a]
26-day decellularised	5.62 ± 1.51[b] (0.011)	4.08 ± 0.55[b] ($p < 0.001$)	8.74 ± 1.15[b] ($p < 0.001$)	6.87 ± 0.48[a] (0.313)	94.15 ± 9.56[b] (0.006)
4-day decellularised	11.00 ± 2.73[a] (0.788) [0.039]	4.20 ± 1.11[b] ($p < 0.001$) [0.992]	10.66 ± 2.18[b] (0.001) [0.663]	7.03 ± 0.67[a] (0.532) [0.908]	119.61 ± 11.74[a] (0.822) [0.019]

Between 26-day decellularised and native groups, significant differences were determined for E_0, E_1, E_2 and τ_2. Between 4-day decellularised and native groups, the time-dependent moduli E_1 and E_2 were found to significantly differ. Between 26-day and 4-day decellularised groups, significant differences were determined for E_0 and τ_2.

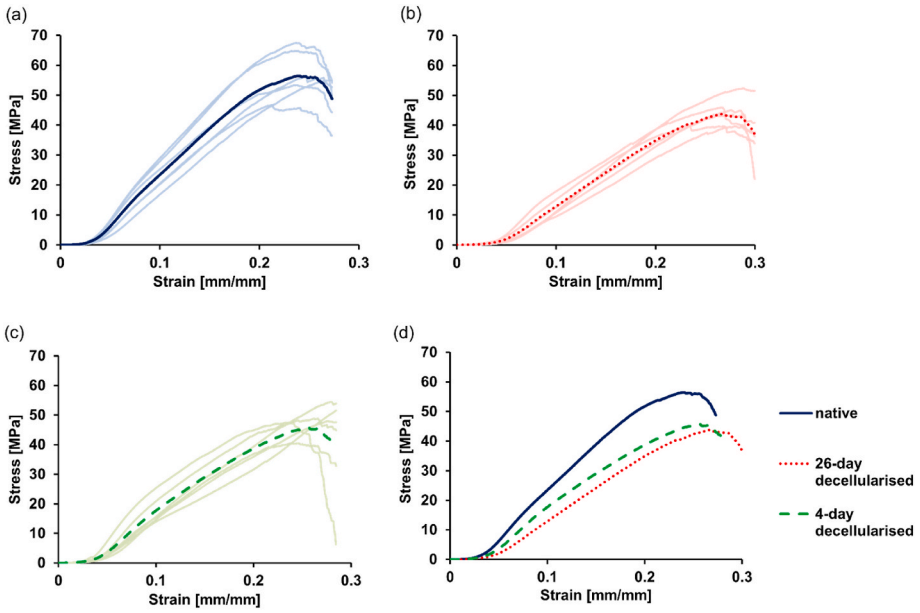

Fig. 4. Mean stress-strain profiles obtained during failure testing for **(a)** native, **(b)** 26-day decellularised and **(c)** 4-day decellularised pSFT groups (n = 6 in all cases). All specimen curves for each group are shown with the mean curve highlighted in bold. **(d)** The mean curves are reproduced in isolation to compare groups.

the solid elastic properties of tissue (Jimenez Rios et al., 2007). E_0 for the 4-day group was not found to be significantly different (unlike the 26-day group) to the native, indicating that the shorter process is less damaging to the extracellular matrix and maintains elastic recovery similar to native tissue.

Following failure testing, the decellularisation protocols for 26-day and 4-day groups appeared to have a similar effect on their stress-strain profiles (see Fig. 4), with a lower UTS and a significant reduction in linear region modulus, E_{linear}. The 26-day group was found to have four out of eight parameters significantly different to native tissue, P_{FAIL}, UTS, E_{linear} and ε_T. The 4-day group was found to have one out of eight parameters significantly different to native tissue, E_{linear} (Table 2). The toe region of the stress-strain curve is indicative of the transformation of the collagen fibres from crimped to straight orientations (Herbert et al., 2016). For the 26-day group, the transition strain, ε_T, which is positioned at the transition from the toe region to the linear region, increased significantly compared to the native tissue group, perhaps indicating some changes to the crimping of the collagen fibres. It has been suggested that alterations in the crimp period caused by the decellularisation process reduce the initial stiffness of tendons (Herbert

Table 2
Tensile testing parameters determined from failure testing for native, 26-day and 4-day decellularised pSFT groups. All data is presented as mean ± 95 % confidence intervals (n = 6). One-way ANOVA with Tukey post-hoc test to determine significant differences ($p < 0.05$). Groups not sharing the same superscript letter within each column are significantly different. Values in round brackets indicate p-value when 26- and 4-day decellularised groups are compared to the native group. Values in square brackets indicate p-values when comparing 26- and 4-day decellularised groups.

Group	P_{FAIL} [N]	UTS [MPa]	ε_{FAIL} [mm mm^{-1}]	E_{toe} [MPa]	E_{linear} [MPa]	ε_T [mm mm^{-1}]	σ_T [MPa]	δ_{FAIL} [mm]
Native	941.28 ± 87.28[a]	57.29 ± 6.13[a]	0.24 ± 0.02[a]	16.54 ± 6.92[a]	326.33 ± 33.01[a]	0.03 ± 0.01[a]	0.57 ± 0.31[a]	9.71 ± 1.03[a]
26-day decellularised	740.37 ± 80.38[b] (0.009)	44.40 ± 3.74[b] (0.006)	0.27 ± 0.02[a] (0.078)	18.90 ± 6.35[a] (0.863)	230.98 ± 21.65[b] (0.001)	0.05 ± 0.01[b] (0.020)	0.96 ± 0.40[a] (0.261)	10.56 ± 0.56[a] (0.052)
4-day decellularised	792.75 ± 73.70[a, b] (0.054) [0.648]	49.11 ± 4.37[a, b] (0.081) [0.393]	0.26 ± 0.02[a] (0.234) [0.796]	17.26 ± 5.58[a] (0.986) [0.931]	251.86 ± 27.88[b] (0.006) [0.566]	0.04 ± 0.01[a, b] (0.704) [0.091]	0.66 ± 0.27[a] (0.931) [0.429]	10.17 ± 0.98[a] (0.189) [0.721]

Between the 26-day decellularised and native groups, significant differences were determined for P_{FAIL}, UTS, E_{linear} and ε_T. The only parameter found to significantly differ between 4-day decellularised and native groups was E_{linear}. Between 26-day and 4-day decellularised groups no significant differences were found.

et al., 2015). As a result, greater strain is required to achieve stresses equivalent to those of native tendons. These modifications in the toe region are consistent with the observed changes in collagen crimp morphology identified through Picro-Sirius Red staining (Fig. 2 I).

The failure testing followed established protocols previously implemented by our group (Herbert et al., 2015; Jones et al., 2017). While the UTS of native pSFT was found to be similar, some mechanical properties exhibited variations, such as the strain at failure, ϵ_{FAIL}, which was lower at 0.24 mm mm^{-1} compared to previously reported values of 0.32–0.33 mm mm^{-1} and the linear region modulus, E_{linear}, which was higher in this study at 326 MPa compared to previously reported values of 234–235 MPa (Herbert et al., 2015; Jones et al., 2017). These discrepancies may be attributed to variations in experimental conditions, including freezing of the tissue during the testing due to the use of dry ice in cyroclamps, PBS induced swelling and differences in cross-sectional area measurement techniques. The maximum force, P_{FAIL} and extension at failure, δ_{FAIL} of the 26-day decellularised tissue remained within a comparable range to those reported in previous studies by our group (Herbert et al., 2015; Jones et al., 2017).

To prevent macroscopic damage that could lead to graft failure, it is essential that the physiological loads experienced by the implanted tendon graft remain within the linear elastic region (Sensini and Cristofolini, 2018). Both native and decellularised pSFT exhibited a significantly higher linear region modulus (Young's modulus) than the human ACL (Noyes and Grood, 1976; Marieswaran et al., 2021; Chandrashekar et al., 2006). However, direct comparison with literature values is challenging due to differences in applied strain rates and donor age variability in human tissue. The UTS of both native and decellularised pSFT (44–57 MPa) exceeded reported values for the human ACL (9–38 MPa) (Noyes and Grood, 1976; Woo et al., 1991; Marieswaran et al., 2021; Chandrashekar et al., 2006; Jones et al., 1995; Trent et al., 1976). Following implantation, the graft is expected to undergo an initial period of degradation, resulting in a reduction in Young's modulus prior to constructive remodelling occurring (Hunt et al., 2025). Therefore, it is crucial that the tendon graft initially possesses greater Young's modulus and strength than the human ACL, to compensate for this structural weakening. However, while autografts undergo early degeneration as a result of local cell death, decellularised grafts are expected to exhibit reduced degeneration owing to the absence of viable cells.

Previous studies estimate that the peak forces applied to the ACL during activity range from approximately 250-300 N (Hosseini et al., 2011; Shelburne et al., 2004), corresponding to a stress of 4–5 MPa, which is significantly lower than the failure thresholds of both the ACL and the native and decellularised pSFT. However, these estimates may be conservative for individuals engaged in high-impact sports, as research on dynamic and multi-axial loading of the ACL remains limited. Since both the 26-day and 4-day decellularised tendons exhibited greater Young's modulus and UTS than the human ACL, they are mechanically robust and should not rupture immediately after implantation.

The mechanical testing results demonstrate that failure testing in isolation is insufficient to characterise changes in the biological tissue, highlighting the need to also assess the viscoelastic properties. Stress relaxation testing provides a more representative evaluation of how the tendon graft will be loaded and recover under physiological conditions. Previous research has noted the importance of maintaining the native microenvironment of the scaffolds extracellular matrix, as key signalling proteins may be lost during the decellularisation process (Moffat et al., 2022; Ohata and Ott, 2020). These proteins play a crucial role in modulating immune responses, promoting cell proliferation and graft regeneration. This study demonstrates that a 4-day decellularisation process better preserves the mechanical properties of the graft compared to the original 26-day process, suggesting that tendons decellularised using the 4-day process may provide enhanced cell migration and accelerate post-implantation healing.

The discovery of a more efficient decellularisation process not only reduces manufacturing costs but also enables greater research productivity by streamlining experimental workflows. The 4-day process is particularly well-suited for industrial settings as its completion within a single workweek improves scalability. Additionally, the simplified protocol facilitates automation, further increasing consistency and production output.

There are limitations to this study, one of which is the use of a simplified experimental environment that does not fully replicate the complex biomechanical conditions of the knee. Additionally, the study focuses solely on uniaxial loading in the direction of the fibres of the tissue, whereas the ACL is also subjected to shear and torsion in-vivo (Marieswaran et al., 2018). The porcine hind leg was stored for up to 3 days in chilled conditions prior to dissection of the tendon, which could result in some initial degradation. However, any such effects would have been equally present in all tendon groups investigated. Furthermore, the chosen sample size ($n = 6$) limits the statistical power, making it possible to detect only large differences between groups. Literature indicates a sample size of six is sufficient when using similar animal tissue models due to consistency in animal age, weight and diet (Serdar et al., 2021). This sample size has also been used in previous research of porcine tendons (Solis-Cordova et al., 2023; Edwards et al., 2017, 2019, 2021; Herbert et al., 2015, 2017; Whitaker et al., 2019; Jones et al., 2017).

There are several key areas for future research, including a more detailed investigation into the reduction of tissue component structural alterations with the 26-day process versus the 4-day process using atomic force microscopy, as well as studies on effects on cell migration and in-vivo implantation to assess long-term integration and functionality.

5. Conclusion

The 4-day decellularisation process better preserves the native properties of porcine flexor tendon tissue compared to the 26-day process, particularly in terms of viscoelastic behaviour, as determined by stress relaxation testing. This suggests a reduced impact on the extracellular matrix, potentially retaining key signalling proteins that facilitate healing. Additional benefits include the development of a shorter process that enhances research productivity, lowers manufacturing cost and a process that lends itself to industry by being completed in a single work week with the possibility of automation.

CRediT authorship contribution statement

Victoria Haines: Writing – review & editing, Writing – original draft, Visualization, Project administration, Methodology, Investigation, Formal analysis, Data curation, Conceptualization. **Jennifer Helen Edwards:** Supervision, Resources, Project administration, Methodology, Conceptualization. **Anthony Herbert:** Writing – review & editing, Supervision, Resources, Project administration, Methodology, Funding acquisition, Conceptualization.

Funding sources

This research was funded through the Faculty of Engineering and Physical Sciences EPSRC DTP, EP/W524372/1 and in affiliation with the Bragg Centre for Materials.

Declaration of competing interest

The authors declare that they have no known competing financial interests or personal relationships that could have appeared to influence the work reported in this paper.

Acknowledgements

The authors thank Nicola Conway for expertise and assistance on histology.

Data availability

The data associated with this paper are openly available from the University of Leeds Data Repository (https://doi.org/10.5518/1802).

References

Aeberhard, P.A., Grognuz, A., Peneveyre, C., McCallin, S., Hirt-Burri, N., Antons, J., Pioletti, D., Raffoul, W., Applegate, L.A., 2020. Efficient decellularization of equine tendon with preserved biomechanical properties and cytocompatibility for human tendon surgery indications. Artif. Organs 44 (4), E161–E171.

Chandrashekar, N., Mansouri, H., Slauterbeck, J., Hashemi, J., 2006. Sex-based differences in the tensile properties of the human anterior cruciate ligament. J. Biomech. 39 (16), 2943–2950.

Crapo, P.M., Gilbert, T.W., Badylak, S.F., 2011. An overview of tissue and whole organ decellularization processes. Biomaterials 32 (12), 3233–3243.

Dayan, D., Hiss, Y., Hirshberg, A., Bubis, J.J., Wolman, M., 1989. Are the polarization colors of picrosirius red-stained collagen determined only by the diameter of the fibers? Histochemistry 93 (1), 27–29.

Dede Eren, A., Sinha, R., Eren, E.D., Huipin, Y., Gulce-Iz, S., Valster, H., Moroni, L., Foolen, J., de Boer, J., 2020. Decellularized Porcine achilles tendon induces anti-inflammatory macrophage phenotype in vitro and tendon repair in vivo. J. Immunol. Regen. Med. 8, 100027.

Dong, S., Huangfu, X., Xie, G., Zhang, Y., Shen, P., Li, X., Qi, J., Zhao, J., 2015. Decellularized versus fresh-frozen allografts in anterior cruciate ligament reconstruction: an in vitro study in a rabbit model. Am. J. Sports Med. 43 (8), 1924–1934.

Edwards, J.H., Herbert, A., Jones, G.L., Manfield, I.W., Fisher, J., Ingham, E., 2017. The effects of irradiation on the biological and biomechanical properties of an acellular porcine superflexor tendon graft for cruciate ligament repair. J. Biomed. Mater. Res. B Appl. Biomater. 105 (8), 2477–2486.

Edwards, J.H., Ingham, E., Herbert, A., 2019. Decellularisation affects the strain rate dependent and dynamic mechanical properties of a xenogeneic tendon intended for anterior cruciate ligament replacement. J. Mech. Behav. Biomed. Mater. 91, 18–23.

Edwards, J.H., Jones, G.L., Herbert, A., Fisher, J., Ingham, E., 2021. Integration and functional performance of a decellularised porcine superflexor tendon graft in an ovine model of anterior cruciate ligament reconstruction. Biomaterials 279, 121204.

Herbert, A., Jones, G.L., Ingham, E., Fisher, J., 2015. A biomechanical characterisation of acellular porcine super flexor tendons for use in anterior cruciate ligament replacement: investigation into the effects of fat reduction and bioburden reduction bioprocesses. J. Biomech. 48 (1), 22–29.

Herbert, A., Brown, C., Rooney, P., Kearney, J., Ingham, E., Fisher, J., 2016. Bi-linear mechanical property determination of acellular human patellar tendon grafts for use in anterior cruciate ligament replacement. J. Biomech. 49 (9), 1607–1612.

Herbert, A., Edwards, J.H., Jones, G.L., Ingham, E., Fisher, J., 2017. The effects of irradiation dose and storage time following treatment on the viscoelastic properties of decellularised porcine super flexor tendon. J. Biomech. 57, 157–160.

Hosseini, A., Gill, T.J., Van de Velde, S.K., Li, G., 2011. Estimation of in vivo ACL force changes in response to increased weightbearing. J. Biomech. Eng. 133 (5), 051004.

Hunt, N., Oliver, G., Borrego, A.F., Pietrzak, W.S., 2025. Five-year clinical study of a novel porcine xenograft for anterior cruciate ligament reconstruction: Positive safety and performance outcomes. J. Exp. Orthop. 12 (3), e70433.

Hussein, K.H., Saleh, T., Ahmed, E., Kwak, H.H., Park, K.M., Yang, S.R., Kang, B.J., Choi, K.Y., Kang, K.S., Woo, H.M., 2018. Biocompatibility and hemocompatibility of efficiently decellularized whole porcine kidney for tissue engineering. J. Biomed. Mater. Res. 106 (7), 2034–2047.

Jimenez Rios, J.L., Steif, P.S., Rabin, Y., 2007. Stress-strain measurements and viscoelastic response of blood vessels cryopreserved by vitrification. Ann. Biomed. Eng. 35 (12), 2077–2086.

Jones, R.S., Nawana, N.S., Pearcy, M.J., Learmonth, D.J., Bickerstaff, D.R., Costi, J.J., Paterson, R.S., 1995. Mechanical properties of the human anterior cruciate ligament. Clin Biomech (Bristol, Avon) 10 (7), 339–344.

Jones, G., Herbert, A., Berry, H., Edwards, J.H., Fisher, J., Ingham, E., 2017. Decellularization and characterization of porcine superflexor tendon: a potential anterior cruciate ligament replacement. Tissue Eng Part A 23 (3–4), 124–134.

Junqueira, L.C., Bignolas, G., Brentani, R.R., 1979. Picrosirius staining plus polarization microscopy, a specific method for collagen detection in tissue sections. Histochem. J. 11 (4), 447–455.

Legnani, C., Ventura, A., 2023. Synthetic grafts for anterior cruciate ligament reconstructive surgery. Med. Eng. Phys. 117, 103992.

Liu, J., Xu, M.Y., Wu, J., Zhang, H., Yang, L., Lun, D.X., Hu, Y.C., Liu, B., 2021. Picrosirius-polarization method for collagen fiber detection in tendons: a mini-review. Orthop. Surg. 13 (3), 701–707.

Maniar, N., Verhagen, E., Bryant, A.L., Opar, D.A., 2022. Trends in Australian knee injury rates: an epidemiological analysis of 228,344 knee injuries over 20 years. Lancet Reg. Health West. Pac. 21, 100409.

Marieswaran, M., Jain, I., Garg, B., Sharma, V., Kalyanasundaram, D., 2018. A review on biomechanics of anterior cruciate ligament and materials for reconstruction. Appl. Bionics Biomech. 2018, 4657824.

Marieswaran, M., Sikidar, A., Rana, A., Singh, D., Mansoori, N., Lalwani, S., Kalyanasundaram, D., 2021. A cadaveric study on the rate of strain-dependent behaviour of human anterior cruciate ligament. Acta Bioeng. Biomech. 23 (1), 45–57.

Moffat, D., Ye, K., Jin, S., 2022. Decellularization for the retention of tissue niches. J. Tissue Eng. 13, 20417314221101151.

Nordenvall, R., Bahmanyar, S., Adami, J., Stenros, C., Wredmark, T., Fellander-Tsai, L., 2012. A population-based nationwide study of cruciate ligament injury in Sweden, 2001-2009: incidence, treatment, and sex differences. Am. J. Sports Med. 40 (8), 1808–1813.

Nordin, M., Frankel, V.H., 2022. Basic Biomechanics of the Musculoskeletal System, fifth ed. Wolters Kluwer.

Noyes, F.R., Grood, E.S., 1976. The strength of the anterior cruciate ligament in humans and Rhesus monkeys. J. Bone Joint Surg. Am. 58 (8), 1074–1082.

Ohata, K., Ott, H.C., 2020. Human-scale lung regeneration based on decellularized matrix scaffolds as a biologic platform. Surg. Today 50 (7), 633–643.

Riemersa, D.J., Schamhardt, H.C., 1982. The cryo-jaw, a clamp designed for in vitro rheology studies of horse digital flexor tendons. J. Biomech. 15 (8), 619–620.

Saueressig, T., Braun, T., Steglich, N., Diemer, F., Zebisch, J., Herbst, M., Zinser, W., Owen, P.J., Belavy, D.L., 2022. Primary surgery versus primary rehabilitation for treating anterior cruciate ligament injuries: a living systematic review and meta-analysis. Br. J. Sports Med. 56 (21), 1241–1251.

Sensini, A., Cristofolini, L., 2018. Biofabrication of electrospun scaffolds for the regeneration of tendons and ligaments. Materials (Basel) 11 (10).

Serdar, C.C., Cihan, M., Yucel, D., Serdar, M.A., 2021. Sample size, power and effect size revisited: simplified and practical approaches in pre-clinical, clinical and laboratory studies. Biochem Med (Zagreb) 31 (1), 010502.

Shelburne, K.B., Pandy, M.G., Anderson, F.C., Torry, M.R., 2004. Pattern of anterior cruciate ligament force in normal walking. J. Biomech. 37 (6), 797–805.

Solis-Cordova, J., Edwards, J.H., Fermor, H.L., Riches, P., Brockett, C.L., Herbert, A., 2023. Characterisation of native and decellularised porcine tendon under tension and compression: a closer look at glycosaminoglycan contribution to tendon mechanics. J. Mech. Behav. Biomed. Mater. 139, 105671.

The_National_Ligament_Registry, The Seventh Annual Report, 2022.

Trent, P.S., Walker, P.S., Wolf, B., 1976. Ligament length patterns, strength, and rotational axes of the knee joint. Clin. Orthop. Relat. Res. (117), 263–270.

Whitaker, S., Edwards, J.H., Guy, S., Ingham, E., Herbert, A., 2019. Stratifying the mechanical performance of a decellularized xenogeneic tendon graft for anterior cruciate ligament reconstruction as a function of graft diameter: an animal study. Bone Joint Res. 8 (11), 518–525.

Woo, S.L., Hollis, J.M., Adams, D.J., Lyon, R.M., Takai, S., 1991. Tensile properties of the human femur-anterior cruciate ligament-tibia complex. The effects of specimen age and orientation. Am. J. Sports Med. 19 (3), 217–225.

Zbrojkiewicz, D., Vertullo, C., Grayson, J.E., 2018. Increasing rates of anterior cruciate ligament reconstruction in young Australians, 2000-2015. Med. J. Aust. 208 (8), 354–358.